A SOLAR IRON ABUNDANCE DETERMINATION USING LINES IN THE NEAR UV

* NSG-438

Scientific Report No. 17

By

George L. Withbroe

Harvard College Observatory

March 1967

ABSTRACT

Lines of Fe I located between 3100 and 3800 Å are used to determine the solar iron abundance. We find an abundance that is a factor of four smaller than the photospheric abundance determined from lines in the visible part of the spectrum. Possible explanations for this apparent discrepancy are discussed.

I. INTRODUCTION

One of the problems of solar physics is the determination of accurate solar abundances. For elements such as Be, Ru, Rh, Pd, Ag, Cd, Sn, and Pb this is difficult because most or all of the relevant spectral lines fall in the wavelength region between 3000 and 4000 Å. There are two basic difficulties in using lines in the near UV for determining abundances: (1) This spectral region is so crowded with spectral lines that the continuum is poorly defined. (2) The continuous absorption coefficient is not as well known as it is in the visible part of the solar spectrum. In this paper we shall use new observations of a number of lines of Fe I to study these problems.

II. OBSERVATIONS

The observations are from an "Atlas of the Solar Spectrum from 3000 to 7500 Å " (Delbouille, Roland, and Neven, to be published). These observations were made with photoelectric equipment at the Jungfraujoch Scientific Station. We are indebted to Dr. Delbouille and his colleagues for sending us

copies of tracings covering a large fraction of the UV portion of the atlas prior to publication. The tracings were made with significantly higher spectral resolution than that found in Brückner's UV atlas (Brückner 1960). We measured the equivalent widths of 71 Fe I lines from the tracings. In almost all cases we used a local continuum defined by the highest level of intensity within one or two Ångstroms of the Fe I line. For a few lines located on the wings of very strong lines we drew in the expected shape of the wing of the strong line and used this extrapolated wing as our local continuum. One of the objectives of this analysis is the determination of the reliability of this procedure. The measured equivalent widths are given in Table I.

In Fig. 1 we have compared our equivalent widths with those given in the Utrecht atlas (Utrecht 1960). The degree of scatter of the points about the 45° line illustrates the difficulty of obtaining accurate equivalent widths for individual spectral lines in the near UV solar spectrum. There appear to be no significant differences between the two sets of measurements.

III. THEORY

In the calculation of theoretical equivalent widths we used

the method of weighting functions. We computed the line depth, r, using a procedure very similar to that used by Aller, Elste and Jugaku (1957). At the center of the solar disc the line depth is given by

$$r(\Delta\lambda) = \frac{I_\lambda - I_\ell(\Delta\lambda)}{I_\lambda} = \int_0^\infty \frac{\kappa_\ell}{\kappa_\lambda}(\Delta\lambda)\ \exp\left[-\int_0^{\tau_\lambda} \frac{\kappa_\ell}{\kappa_\lambda}(\Delta\lambda)\ dt\right] g_\lambda(\tau_\lambda)\ d\tau_\lambda\ , \qquad (1)$$

where I_λ is the emergent intensity in the continuum, $I_\ell(\Delta\lambda)$ is the emergent intensity in the line at a distance $\Delta\lambda$ from the center of the line, κ_λ is the continuous absorption coefficient per hydrogen particle, and g_λ is the weighting function (e.g. Aller 1960). The line absorption coefficient, κ_ℓ, is proportional to $(N_E/N_H)\cdot(N_{r,s}/N_E)$ where N_E/N_H is the solar abundance of element E with respect to hydrogen, and $N_{r,s}$ is the number of atoms per cm^3 in the lower level of the transition. The quantity $N_{r,s}/N_E$ may be expressed as a function of the photospheric electron temperature and pressure by using Boltzmann's and Saha's equations.

The equivalent widths were evaluated from the formula:

$$W_\lambda = \int_{-\infty}^{\infty} r(\Delta\lambda)\cdot d(\Delta\lambda)\,. \qquad (2)$$

The equivalent width of a weak line can be related to the solar abundance, N_E/N_H , by an equation of the form:

$$\log W_\lambda/\lambda = \log C_\lambda + \log N_E/N_H \quad , \tag{3}$$

(e.g. Müller and Mutschlecner 1964) where

$$\log C_\lambda = \log gf\lambda + \theta_o \Delta\chi + \log C_\lambda' \quad ; \tag{4}$$

g is the statistical weight of the lower level of the transition; f is the oscillator strength of the line; λ is the wavelength; $\Delta\chi$ is the difference between the ionization potential of element E and the excitation potential of the lower level of the transition; and C_λ' depends upon the photospheric model, $\varkappa_\lambda$, and the ionization properties of the element. The quantity $\theta_o = 5040/T_o$ may be taken as unity for the sun, T_o representing a mean temperature in the atmospheric layers where the lines are formed.

An empirical curve-of-growth is obtained by plotting the observed values of $\log W_\lambda/\lambda$ as a function of $\log C_\lambda$. By comparing theoretical and empirical curves-of-growth one can obtain a value for $\log N_E/N_H$.

It is important to note that C_λ' depends upon the depth-

dependence of the continuous absorption coefficient, κ_λ . We indicated in the Introduction that κ_λ is not as well known in the UV as it is in the visible. There is evidence for the existence of an additional source or sources of opacity besides the usual hydrogenic sources for wavelengths shorter than 4500 Å (Pierce and Waddell 1961, David 1961). It appears possible that this additional opacity may be caused by bound-free transitions in the metallic elements. As a first approximation one may use the hydrogenic approximation to express the metallic absorption coefficient in terms of the photospheric electron temperature and pressure. We have for each metallic element (Unsöld 1955):

$$\kappa_\lambda/\text{ion} = \frac{16\,\pi^2}{3\sqrt{3}} \frac{e^6\,(Z+s)^2}{ch(2\pi mk)^{3/2}} \frac{P_e}{T^{3/2}} \exp\left(\frac{hc}{\lambda kT}\right)\left(\frac{\lambda}{c}\right)^3 , \qquad (5)$$

where P_e is the electron pressure, T is the electron temperature, (Z+s) is the effective nuclear potential, and the other parameters are atomic constants. In our initial computations we followed Vitense (1951) and assumed $(Z+s)^2 = 4$ for all the metals. The total absorption coefficient, κ_λ , was obtained by summing the contributions of the metals, atomic hydrogen, H^- , H_2^+ , electron scattering, and Rayleigh scattering from atomic hydrogen.

IV. PHOTOSPHERIC MODEL

The photospheric model that we have used was derived by Mutschlecner (Müller and Mutschlecner 1964). The depth dependences of the electron temperature and pressure in Mutschlecner's model are given in Table 2. Müller and Mutschlecner were able to explain successfully with this model the center-limb behavior of spectral lines in the iron group of elements. The model also has been used by Goldberg, Kopp, and Dupree (1964) in a determination of the solar abundance of iron.

One problem that arises in using this model is that the layers at optical depths smaller than log $\tau_{5000} = -3.6$ contribute significantly to the intensities in the cores of the stronger Fe I lines. We avoided this difficulty by extending the model to log $\tau_{5000} = -5.0$ keeping the temperature in these layers equal to the temperature at log $\tau_{5000} = -3.6$.

V. THE OSCILLATOR STRENGTHS

The gf-values used in our analysis are from Huber and Tobey (1967) and Corliss and Warner (1964, 1966). The

The gf-values of Huber and Tobey are based upon measurements made in a shock tube at the Harvard Shock Tube Spectroscopy Laboratory. Since the physical conditions in a shock tube can be accurately determined, these gf-values should be reliable on both a relative and an absolute scale. The relevant gf-values taken from the tables of Corliss and Warner are based upon measurements of several different investigators. These measurements were normalized to the absolute scale of Corliss and Bozman (1962).

In Fig. 2 we have compared the gf-values of Huber and Tobey with those of Corliss and Warner. On a relative scale the agreement is good, however, on an absolute scale the agreement is poor. The gf-values of Huber and Tobey are systematically smaller than those of Corliss and Warner by 0.8 dex ($0.8 \text{ dex} = 10^{0.8}$). Since the more recent determinations of the solar abundance of iron are based on the absolute scale used by Corliss and Warner, we have corrected the gf-values of Huber and Tobey to this scale. Whenever possible we used the corrected values of Huber and Tobey in our analysis (29 lines). For the remainder of the lines (42 lines) we used the values of Corliss and Warner.

VI. DISCUSSION

In Fig. 3 we have plotted as a function of log C_λ the observed values of log W_λ/λ of the UV lines of Fe I. For comparison we have plotted in Fig. 4 similar values for Fe I lines in the 4000 to 7000 Å region. The equivalent widths of the latter lines were taken from Müller and Mutschlecner (1964). The gf-values were obtained from the tables of Corliss and Warner (1964). We have passed a theoretical curve-of-growth through each set of observations. The theoretical curves were computed for an isotropic depth-independent microturbulence with a magnitude of 1.8 km/sec. The UV equivalent widths were fitted to a curve-of-growth computed for 3500 Å; the other set of equivalent widths were fitted to a curve computed for 5000 Å.

We see that the scatter of the observed points about the best fitting theoretical curves is similar in both spectral regions. There is, however, one major difficulty. Although we used the same photospheric model, turbulence model, and absolute scale of gf-values for both sets of observations, we found that log $N_{Fe}/N_H = -5.3$ for the observations of Müller and Mutschlecner while log $N_{Fe}/N_H = -5.9$ for the UV observations.

We found a similar wavelength dependence in the solar iron abundance when the Utrecht UV equivalent widths were used. This is rather disturbing, since both the UV and the visible Fe I lines fall on the same part of the curve-of-growth.

We might mention at this point that Huber and Tobey (1967) found evidence that the normalization function defining the absolute scale used by Corliss and Warner (1966) is incorrect for spectral lines produced by transitions from upper levels with energies, E_u, greater than 5.95 volts. This normalization function causes the gf-values of lines with $E_u > 5.95$ volts to be reduced with respect to gf-values of lines with $E_u < 5.95$ volts. Following the suggestion of Huber and Tobey we renormalized the UV gf-values of Corliss and Warner by using the same normalization function for lines with $E_u > 5.95$ volts as was used for lines with $E_u < 5.95$ volts. The renormalized gf-values are larger than the corresponding values of Huber and Tobey by 0.9 dex. As is illustrated in Fig. 5 the use of the corrected gf-values reduces the scatter in the UV curve-of-growth slightly. It also reduces the UV iron abundance by 0.15 dex. This increases the difference between the abundance determined from lines in the UV and the visible.

There are two ways of explaining this apparent abundance discrepancy: (1) The wavelength dependence in the solar abundance of iron may be caused by the fact that our solar model does not adequately represent the physical conditions in the solar photosphere. (2) There may be a wavelength-dependent error in the gf-values. Let us consider these possibilities in more detail.

The solar model could be inadequate in a number of ways. For example, the theoretical continuum used in calculating the curves-of-growth may not correspond to the local continuum used in measuring the empirical equivalent widths. Since the spectral region between 3000 and 4000 Å is very crowded with spectral lines, the overlapping wings of the lines may depress the local continuum with respect to the true continuum. The true continuum is the continuum that would be observed if no spectral lines were present. It is identical to the continuum used for the theoretical curves-of-growth.

In order to study the influence of the depression of the continuum on the UV iron abundance we did the following: We added to the line absorption coefficent, κ_ℓ, an additional opacity with the same depth dependence as the absorption coefficent of a typical iron line. By varying the amount of this additional

opacity we could depress the local continuum with respect to the true continuum by any arbitrary amount. In Fig. 6 we have plotted theoretical curves-of-growth calculated for different values of I_L/I_C where I_L is the intensity of the local continuum and I_C is the intensity of the true continuum. The equivalent widths of the lines making up the curves-of-growth were measured with respect to I_L. The iron abundance assumed was the value determined from iron lines in the visible, $\log N_{Fe}/N_H = -5.3$. We see that the Fe I curve-of-growth is relatively insensitive to changes in I_L/I_C and that I_L/I_C would have to be improbably small, 0.3 to 0.4, in order to explain the equivalent widths of the UV iron lines.

We also computed several small regions of the UV solar spectrum for wavelengths shorter than the Balmer limit at 3647 Å, representing each observed spectral line by an iron line of the same equivalent width. We found that the height of the theoretical local continuum was close to the height of the true continuum for spectral regions similar to those where the Fe I lines in Table 1 are located. This result along with that described in the previous paragraph indicates that the depression of the continuum is unimportant for Fe I lines with $\lambda < 3647$. In the spectral region longward of the Balmer limit

the continuum is definitely depressed by the overlapping wings of the Balmer lines. However, calculations similar to those described above indicate that this does not have a significant effect on the theoretical equivalent widths of the Fe I lines as long as one measures with respect to the local continuum.

We conclude from these results that it is unlikely that the depression of the continuum by the overlapping wings of spectral lines affects the equivalent widths of the UV iron lines enough to explain the small UV iron abundance.

Another way that the solar model could be inadequate is that the assumed continuous absorption coefficient is incorrect. In the initial computations we included a metallic contribution to the total UV opacity. We estimated the magnitude of the metallic contribution by using the hydrogenic approximation (equation 5) and assuming $(Z+s)^2 = 4$. Since this estimate could be in error by an order of magnitude, we calculated curves-of-growth using a variety of values for $(Z+s)^2$. All of the curves were calculated using the iron abundance determined from the Fe I lines in the visible. Three curves are illustrated in Fig. 7. One of these, the curve for $(Z+s)^2 = 120$, fits the observations very well. This suggests that the abundance discrepancy found earlier was caused by the fact that the initial

UV absorption coefficient was too small.

Although this result is encouraging, there are several problems with this explanation. A minor problem is that $(Z+s)^2$ cannot be as large as 120 for all atomic levels contributing significantly to the metallic opacity. If this were the case, the metallic contribution to the opacity would be too large in the visible region of the spectrum. We can avoid this difficulty if we stipulate that the atomic levels contributing to the UV opacity (such as the 4s $^3P^\circ$ level of Si and the 3p $^1P^\circ$ level of Mg) have values of $(Z+s)^2$ an order of magnitude larger than the values of $(Z+s)^2$ for the atomic levels contributing to the opacity in the visible. An alternative solution is that we attribute the extra opacity needed to explain the UV iron abundance to some opacity source other than the metals.

A more difficult problem with the opacity model corresponding to $(Z+s)^2 = 120$ is that it predicts an emergent intensity in the UV smaller than that observed. The theoretical emergent intensity depends upon the depth dependence of the photospheric electron temperature and upon the depth dependence of the continuous absorption coefficient, κ_λ. The depth dependence of the photospheric electron temperature appears to be well determined for the atmospheric layers where the UV continuum is produced. Thus the theoretical emergent intensity depends primarily on the

depth dependence of κ_λ. For the three opacity models used in computing the curves-of-growth in Fig. 7, for which $(Z+s)^2 = 4$, 30, and 120, the theoretical emergent intensities at 3500 Å are $3.8 \cdot 10^{14}$, $2.8 \cdot 10^{14}$, and $1.4 \cdot 10^{14}$ erg/cm^3/sec/sterad/cm respectively. Observed values for this intensity are (in units of 10^{14} erg/cm^3/sec/sterad/cm): 2.9, Mulders (1935); 3.1, Canavaggia et al. (1950); 4.0, Labs (1957); 2.6, Sitnik (1965); and 1.3, Makarova (1965). We see that the opacity models with $(Z+s)^2 = 4$ and $(Z+s)^2 = 30$ give emergent intensities at 3500 Å in good agreement with the observed values. The opacity model with $(Z+s)^2 = 120$ predicts a UV intensity that is a factor of two to three smaller than most observed values.

We should point out that it is difficult to measure accurately the emergent intensity in the UV solar continuum because this spectral region is so crowded with spectral lines. Absolute calibration of UV intensity measurements is also a problem. Because of these problems measurements of UV intensities may be inaccurate. This is borne out by the large scatter in the measured values for the intensity at 3500 Å. For this reason the agreement or disagreement between theoretical and observed UV intensities may not be significant.

Further evidence that the opacity model corresponding to $(Z+s)^2 = 120$ may be incorrect is that the theoretical line

profiles computed with this model are shallower than the observed profiles. For the opacity models with smaller values of $(Z+s)^2$ the theoretical and observed central intensities of the lines are in better agreement. This is illustrated in Fig. 8. We cannot, however, give too much weight to evidence based on the agreement or disagreement between theoretical and observed central intensities. The observed intensities have not been corrected for instrumental broadening or spectrographic scattered light (both of which should be small according to Delbouille), so they are not entirely reliable. The theoretical profiles are affected by the uncertainties in the photospheric model, turbulence model, and possibly departures from LTE. Thus, although the results presented in Fig. 8 are suggestive, they may not be significant.

It is worthwhile to point out here a method of obtaining additional information about the UV continuous absorption coefficent. The theoretical center-limb variation of the equivalent widths of the UV Fe I lines is sensitive to the assumed continuous opacity, as is illustrated for a typical line in Fig. 9. This suggests that an investigation of the center-limb behavior of UV spectral lines would be valuable.

We considered several other ways of explaining the apparent wavelength dependence in the solar iron abundance that we found with our initial opacity model. We examined the possibility that

the neglect of the influence of photospheric inhomogeneities might have caused the abundance discrepancy. In order to test this hypothesis we performed computations with a three stream model developed by G. Elste (1965, unpublished). The depth dependence of the electron temperature in the medium column of this model is very similar to that in Mutschlecner's model. The hot and cool columns of the three stream model are the order of 400° K hotter and cooler respectively than the medium column. This temperature difference is maintained throughout the photosphere. We found that photospheric inhomogeneities as represented by this model do not cause a significant wavelength dependence in the solar iron abundance.

There is also the possibility that departures from LTE might cause a wavelength dependence. However, Müller and Mutschlecner (1964) showed that there is no significant evidence for such departures in the iron group of elements. The UV Fe I lines have excitation energies similar to those used by Müller and Mutschlecner, so we would not expect a non-LTE effect in the UV lines that would not show up in the visible lines.

Another possibility is that the assumed microturbulence model might produce a wavelength dependence in the iron abundance. We checked this for several different microturbulence models and

found that the assumed microturbulence model has a negligible effect on the relative solar abundances determined from Fe I lines in the UV and in the visible.

We conclude that of the different alternatives considered only the model containing the large UV opacity gives an explanation for the small UV iron abundance determined in our initial calculation. Although this opacity model does explain the equivalent widths of the UV Fe I lines, it is not entirely satisfactory. As we have indicated there are two different types of evidence that suggest that this model is incorrect: (1) The emergent UV intensity calculated for this model is two to three times smaller than most observed values. (2) The theoretical profiles of the UV Fe I lines are shallower than the observed profiles. Neither type of evidence is sufficiently strong to enable us to reject the hypothesis that the UV iron abundance can be explained by using an opacity model containing a large non-hydrogenic contribution to the total opacity. However, because this evidence does exist, it is worthwhile to consider an alternative explanation.

Our basic assumption up to this point has been that the apparent wavelength dependence in the solar iron abundance is caused by inadequacies in our original solar model. Another possibility is that there is a wavelength-dependent error in the

gf-values. The absolute scale of the UV gf-values used in this analysis is based on the gf-values of Corliss and Warner (1966). Their gf-values are based in turn upon several sets of measurements that have been reduced to a common absolute scale. Some of these measurements may contain wavelength-dependent errors. Our results indicate that there may be errors of the order of 0.6 dex between gf-values in the UV and in the visible.

It is worthwhile to recall that the absolute UV gf-values of Corliss and Warner are larger by 0.8 dex on the average than the corresponding values of Huber and Tobey. This is consistent with our work which suggests that the UV gf-values of Corliss and Warner may be too large by about 0.6 dex. We conclude that these results raise the question of whether or not there is a wavelength-dependent error in the gf-values of Corliss and Warner.

VII. SUMMARY

One of the problems encountered in the measurement of equivalent widths of lines falling in the solar UV is the problem of determining where to place the continuum. In this investigation we made our measurements with respect to a local continuum. On the basis of our results we suggest that it is

possible to obtain fairly reliable equivalent widths by this procedure.

We calculated theoretical equivalent widths for UV Fe I lines using Mutschlecner's photospheric model, gf-values reduced to the absolute scale of Corliss and Warner, and a solar iron abundance determined from Fe I lines situated in the visible part of the solar spectrum. The resulting theoretical equivalent widths were systematically larger than those observed. The theoretical and observed equivalent widths could be brought into agreement either by increasing the magnitude of the UV continuous absorption coefficient or by decreasing the UV gf-values by about 0.6 dex. Although the solar model with the increased continuous opacity explains the observed equivalent widths of the UV Fe I lines, it gives poor agreement between the theoretical and observed central intensities of the lines. It also predicts an emergent intensity in the UV continuum that is two to three times smaller than most observed values. If the alternative of decreasing the UV gf-values is followed, it is possible to account for the observed equivalent widths and central intensities of the UV Fe I lines and also to explain the observed emergent intensity in the UV continuum. It appears easier to explain existing observations by changing the gf-values than by increasing the continuous opacity. This is evidence

that the gf-values may contain a wavelength-dependent error. However, we cannot rule out the possibility that the gf-values are correct and that either the UV continuous opacity must be increased or that some other parameter not considered may be introducing an apparent wavelength dependence into the solar iron abundance. If the wavelength dependence is caused by an inadequacy in the solar model, then existing solar abundances based on lines between 3100 and 3800 Å may be too small by a factor of two to four.

For future work we suggest that additional measurements be made of the intensity in the UV solar continuum so that we may be able to determine more accurately the magnitude of the UV continuous absorption coefficient. Center-limb observations of the UV Fe I lines would also be useful for this purpose. It would be worthwhile to have additional independent laboratory measurements of absolute gf-values of Fe I lines, particularly UV lines.

Aller, L.H. 1960, Stellar Atmospheres, ed. J.L. Greenstein (Chicago: University of Chicago Press) p. 156.

_____, Elste, G. and Jugaku, J. 1957, Ap. J. Suppl. 3, 1.

Brückner, G. 1960, Photometrischer Atlas des Nahen Ultravioletten Sonnenspektrums 2988 Å - 3629 Å (Gottingen: Vandenhoeck and Ruprecht).

Corliss, C.H. and Bozman, W.R. 1962, "Experimental Transition Probabilities for Spectral Lines of Seventy Elements", NBS Monograph No. 53 (Washington: Government Printing Office).

_____ and Warner, B. 1964, Ap. J. Suppl. 8, 395.

_____ 1966, J. Research NBS 70A, 325.

Canavaggia, R. Chalonge, D., Egger-Moreau, M., and Oziol-Peltey, H. 1950, Ann. d. Ap. 13, 355.

David, K.H. 1961, Z. f. Ap. 53, 37.

Goldberg, L., Kopp, R.A., and Dupree, A.K. 1964, Ap. J. 140, 707.

Huber, M. and Tobey, F.L. 1967, Harvard College Observatory Shock Tube Spectroscopy Laboratory, Scientific Report No. 16.

Labs, D. 1957, Z. f. Ap. 44, 37.

Makarova, E.A. 1965, Soviet A. J. 9, 525.

Mulders, G.F.W. 1935, Z. f. Ap. 11, 132.

Müller, E.A. and Mutschlecner, P.J. 1964, Ap. J. Suppl. 9, 1.

Pierce, A.K. and Waddell, J.H. 1961, Mem. R. A. S. 68, 89.

Sitnik, G.F. 1965, Soviet A.J. 9, 44.

Unsöld, A. 1955, Physik der Sternatmosphären (Berlin: Springer-Verlag), p. 173.

Utrecht 1960,"Preliminary Photometric Catalogue of Fraunhofer Lines λ3164 - λ8770," Rech. Obs. Utrecht, 15.

Vitense, E. 1951, Z. f. Ap. 28, 81.

ACKNOWLEDGEMENTS

I wish to express my appreciation to Dr. L. Delbouille, Dr. G. Roland, and Dr. L. Neven for sending us tracings from their solar atlas. I would like to thank Dr. L. Goldberg, Dr. M.C.E. Huber and Dr. W.H. Parkinson for their helpful comments and suggestions. I would also like to thank Dr. Huber and Dr. F.L. Tobey for the use of their unpublished gf-values.

This work was supported by the National Aeronautics and Space Administration through grant NsG-438 and contract NASw-184.

Table 1. Equivalent Widths of the UV Fe I Lines

λ	X_{ex}	log gf_{HT}	log gf_{CW}	W_λ(mÅ)
3155.291	2.43		-0.55	82.9
3156.272	3.24	-0.05	0.25	109.5
3168.856	2.47	-1.02	-0.32	82.2
3171.356	1.48		-0.86	82.2
3261.340	3.42		-0.26	71.8
3262.022	3.37		-0.14	77.4
3264.525	2.20		-0.36	89.3
3265.055	0.09		-2.18	112.5
3268.243	2.22	-1.35	-0.45	77.0
3278.742	2.42 2.59	-1.24	-0.46	81.5
3280.268	3.30		0.78	90.3
3317.133	2.28	-1.56	-0.60	74.2
3319.258	2.99	-1.10	-0.37	66.3
3322.482	2.94	-0.75	-0.20	101.0
3323.753	2.83		0.29	115.2
3324.545	2.40		-0.39	84.0
3325.479	2.45	-1.41	-0.45	74.5
3331.618	2.43		-0.58	112.0
3351.752	2.73		-0.36	74.0
3354.066	2.86	-1.21	-0.30	77.5
3355.231	3.30		0.55	104.0
3381.354	2.84		-0.62	74.8
3396.981	0.96	-2.46	-1.65	97.2
3401.531	0.91		-1.34	117.8
3402.267	3.24		0.53	111.0
3406.439	3.27	-0.51	0.22	81.5
3406.811	2.22		0.13	136.7
3411.367	2.73		0.01	84.6
3415.541	2.22		-0.29	89.7
3417.269	1.01	-3.19	-2.14	64.7
3418.523	2.22		0.41	122.8
3419.705	2.84		-0.52	83.5
3425.020	3.05		0.42	100.8
3428.758	3.60	-0.43	-0.14	74.2
3437.959	3.27		-0.02	69.7

Table 1 -- Continued

λ	X_{ex}	log gf_{HT}	log gf_{CW}	W_λ (mÅ)
3445.126	2.20		0.57	143.8
3447.286	2.20		0.02	97.7
3450.335	2.22		0.14	123.0
3451.923	2.22		0.15	114.0
3462.358	2.20	-1.91	-1.00	69.1
3463.310	1.48	-2.64	-1.66	64.6
3483.017	0.91	-2.69	-1.97	82.7
3530.392	2.81		0.13	98.3
3531.440	2.43		-1.01	69.2
3543.683	3.41		0.20	80.5
3544.634	2.61	-1.43	-0.55	70.7
3549.872	1.61	-2.26	-1.40	82.4
3595.308	2.87	-0.93	-0.17	80.0
3596.205	2.43	-1.61	-0.84	66.3
3597.048	3.26		-0.21	98.6
3599.632	3.57		0.36	82.5
3625.148	2.83		0.17	111.2
3628.098	2.20	-1.95	-1.11	70.5
3657.137	2.42	-1.68	-0.64	71.5
3659.525	2.45		0.14	99.8
3670.817	2.48	-1.56	-0.75	74.8
3693.032	3.02	-1.13	-0.24	66.2
3695.057	2.59		0.36	107.2
3724.387	2.28		0.22	119.0
3725.496	3.05	-1.33	-0.56	65.2
3752.418	3.04	-1.27	-0.59	71.0
3756.072	2.18	-1.89	-1.10	67.6
3756.943	3.57		0.50	97.5
3760.057	2.40		0.15	115.0
3760.538	2.22		-0.47	102.8
3762.210	3.37	-0.92	-0.69	79.7
3769.996	3.00		-0.40	75.7
3773.699	3.04	-1.20	-0.62	86.1
3774.834	2.22		-0.72	107.3
3777.074	2.99	-1.49	-0.71	66.4
3778.517	3.25		-0.12	78.8

Table 2. Mutschlecner's Photospheric Model

log τ_{5000}	θ=5040/T	P_e	log τ_{5000}	θ=5040/T	P_e
-3.6	1.0944	0.1323×10^{0}	-1.0	0.9705	0.3554×10^{1}
-3.4	1.0938	0.1647×10^{0}	-0.8	0.9400	0.5304×10^{1}
-3.2	1.0933	0.2044×10^{0}	-0.6	0.9070	0.8479×10^{1}
-3.0	1.0925	0.2538×10^{0}	-0.4	0.8703	0.1479×10^{2}
-2.8	1.0913	0.3150×10^{0}	-0.2	0.8290	0.2885×10^{2}
-2.6	1.0894	0.3915×10^{0}	0.0	0.7835	0.6245×10^{2}
-2.4	1.0864	0.4882×10^{0}	0.2	0.7358	0.1437×10^{3}
-2.2	1.0813	0.6127×10^{0}	0.4	0.6845	0.3563×10^{3}
-2.0	1.0748	0.7733×10^{0}	0.6	0.6278	0.9759×10^{3}
-1.8	1.0645	0.9920×10^{0}	0.8	0.5688	0.2788×10^{4}
-1.6	1.0480	0.1307×10^{1}	1.0	0.5038	0.8738×10^{4}
-1.4	1.0253	0.1778×10^{1}	1.2	0.4365	0.2678×10^{5}
-1.2	0.9990	0.2480×10^{1}			

Fig. 1. A comparison of the equivalent widths measured by the author and the Utrecht equivalent widths.

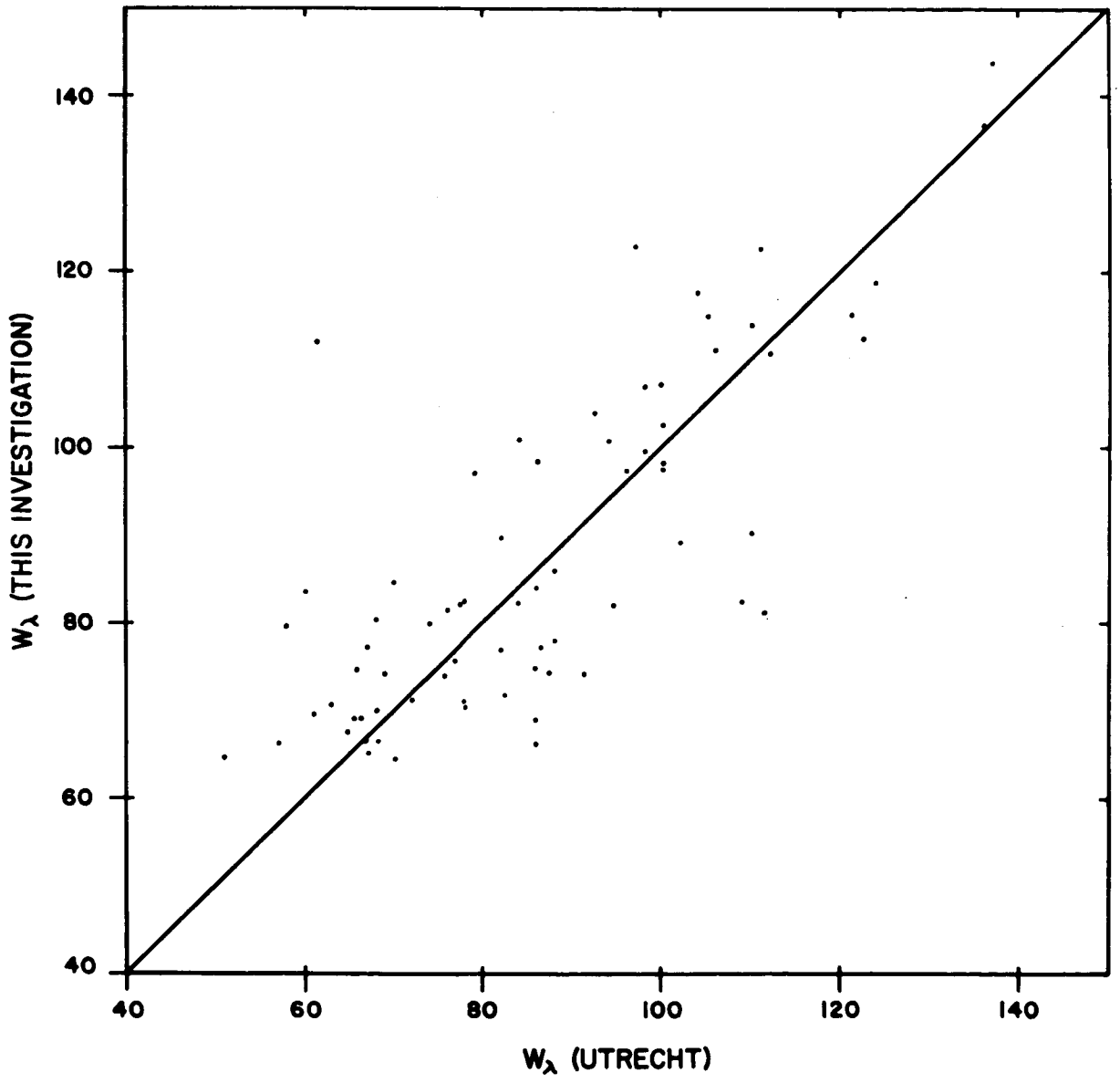
140
120
100
80
60
40
40
60
80
100
120
140
W_λ (THIS INVESTIGATION)
W_λ (UTRECHT)

Fig. 2. A comparison of the gf-values of Huber and Tobey and the corresponding values of Corliss and Warner.

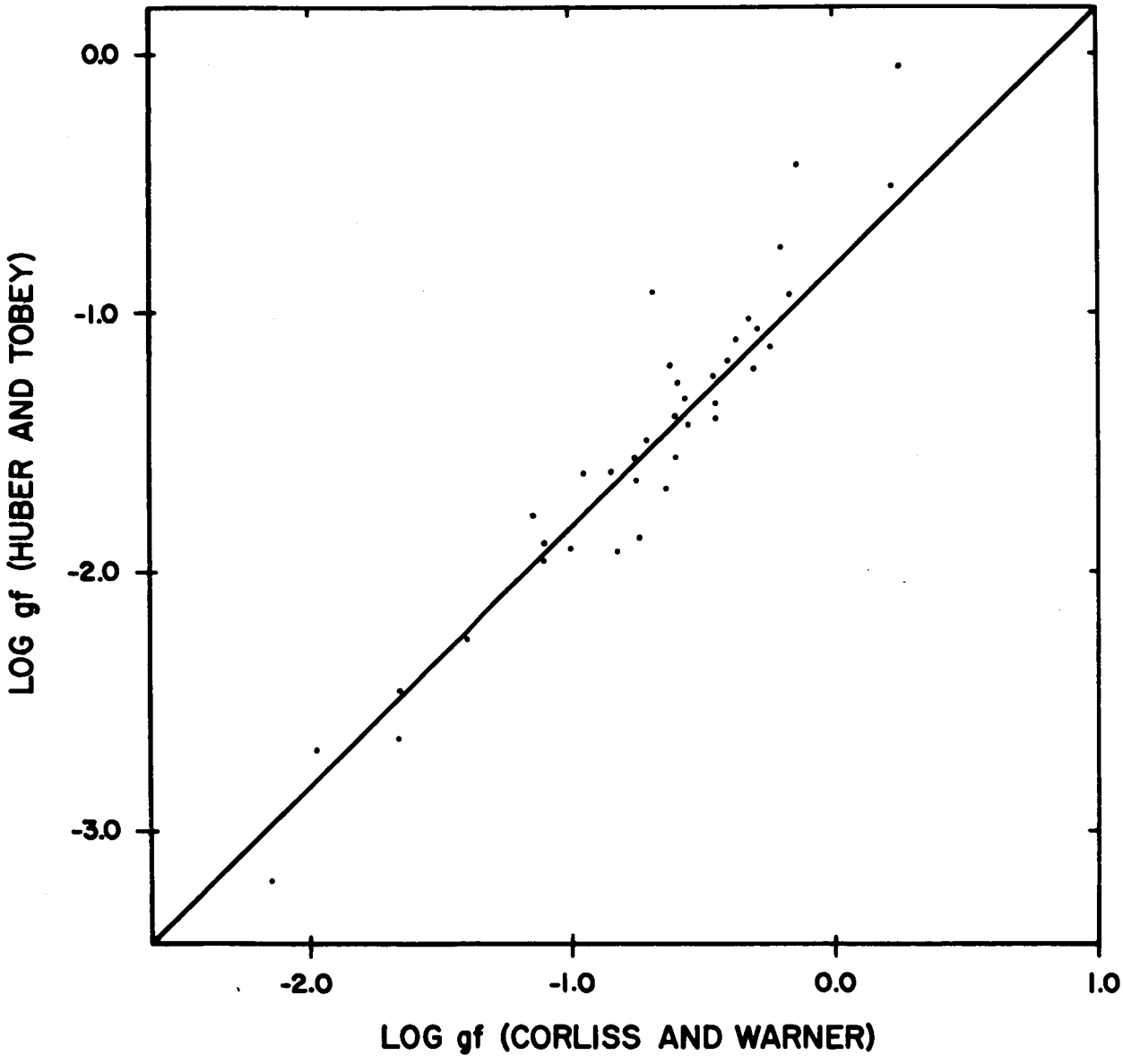
0.0
-1.0
-2.0
-3.0
LOG gf (HUBER AND TOBEY)
-2.0
-1.0
0.0
1.0
LOG gf (CORLISS AND WARNER)

Fig. 3. Curves-of-growth for Fe I lines in the spectral region near 3500 Å.

Crosses: observations, log C_λ computed using the gf-values of Huber and Tobey

Points: observations, log C_λ computed using the gf-values of Corliss and Warner

Solid Line: theoretical curve-of-growth computed for λ = 3500 Å and log N_{Fe}/N_H = -5.3

Dashed Line: curve computed for log N_{Fe}/N_H = -5.9.

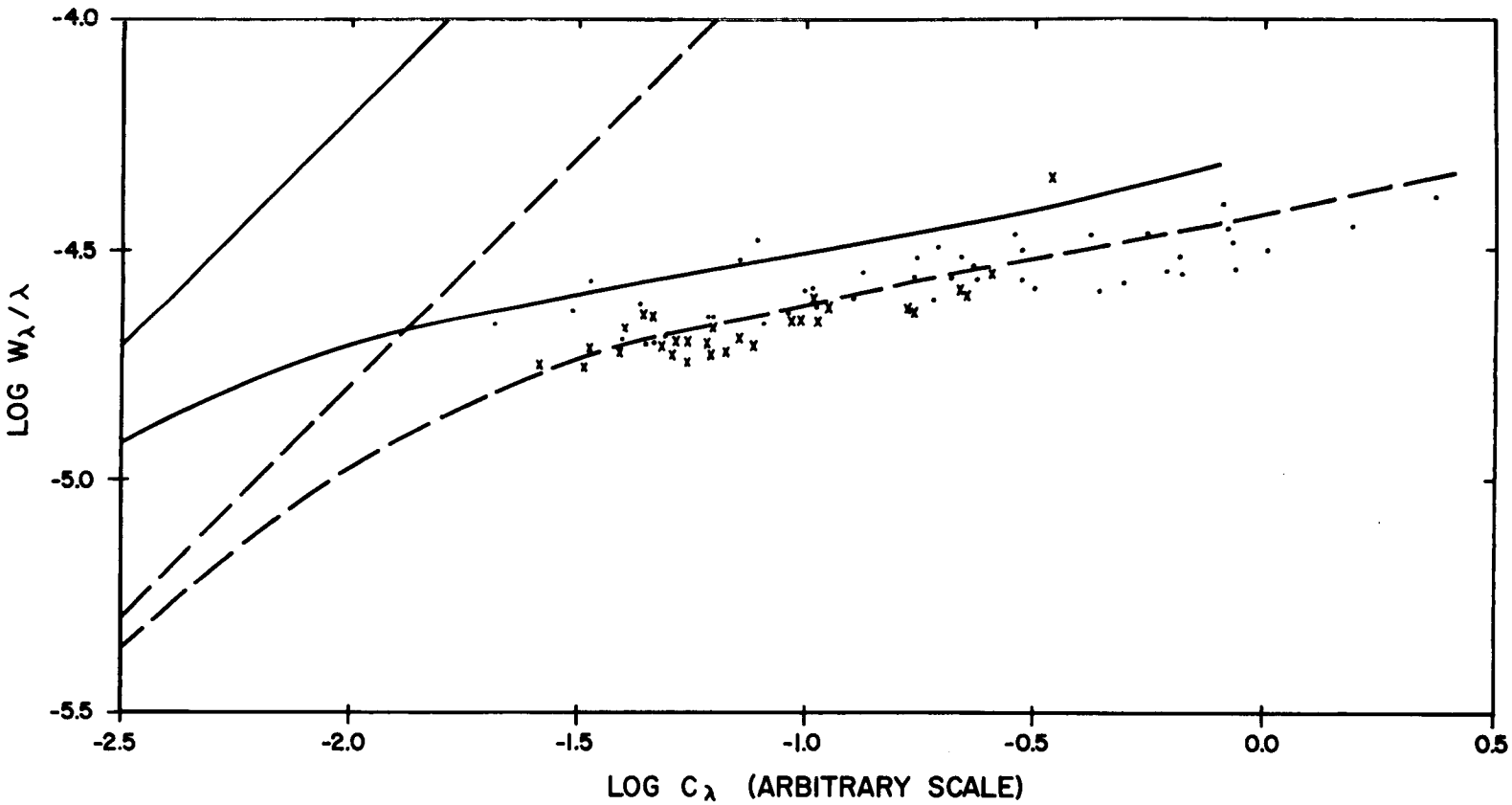
-4.0
-4.5
-5.0
-5.5
LOG W_λ / λ
-2.5
-2.0
-1.5
-1.0
-0.5
0.0
0.5
LOG C_λ (ARBITRARY SCALE)

Fig. 4. Curve-of-growth for the Fe I lines in the visible.

Points: observations

Solid Line: theoretical curve-of-growth computed for $\lambda = 5000$ Å and $\log N_{Fe}/N_H = -5.3$.

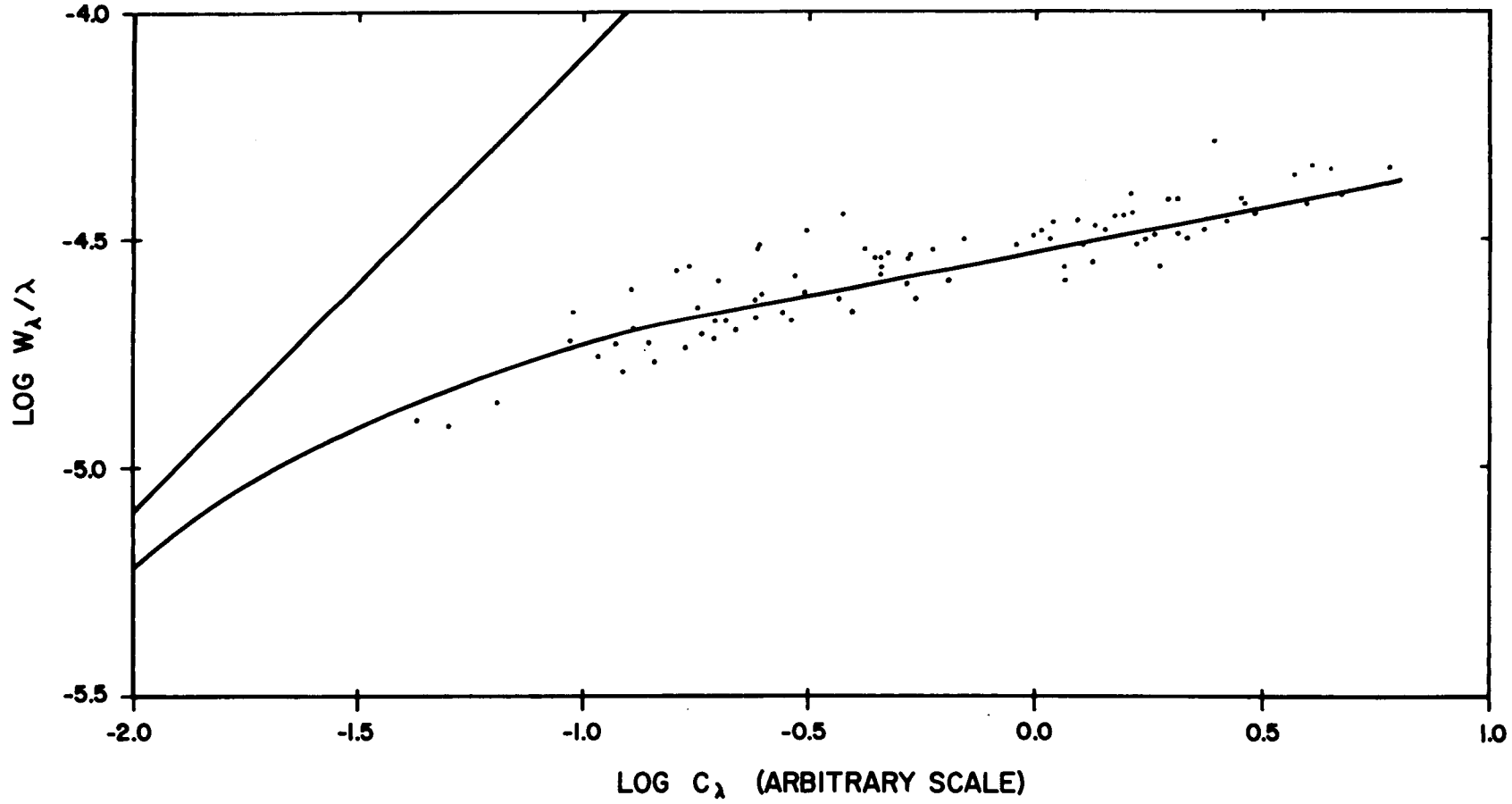
-4.0
-4.5
-5.0
-5.5
LOG W_λ/λ
-2.0
-1.5
-1.0
-0.5
0.0
0.5
1.0
LOG C_λ (ARBITRARY SCALE)

Fig. 5. Curves-of-growth for Fe I lines in the spectral region near 3500 Å.

Crosses: observations, log C_λ computed using the gf-values of Huber and Tobey

Points: observations, log C_λ computed using renormalized gf-values of Corliss and Warner

Solid Line: theoretical curve-of-growth computed for 3500 Å and log $N_{Fe}/N_H = -5.3$

Dashed Line: curve computed for log $N_{Fe}/N_H = -6.05$.

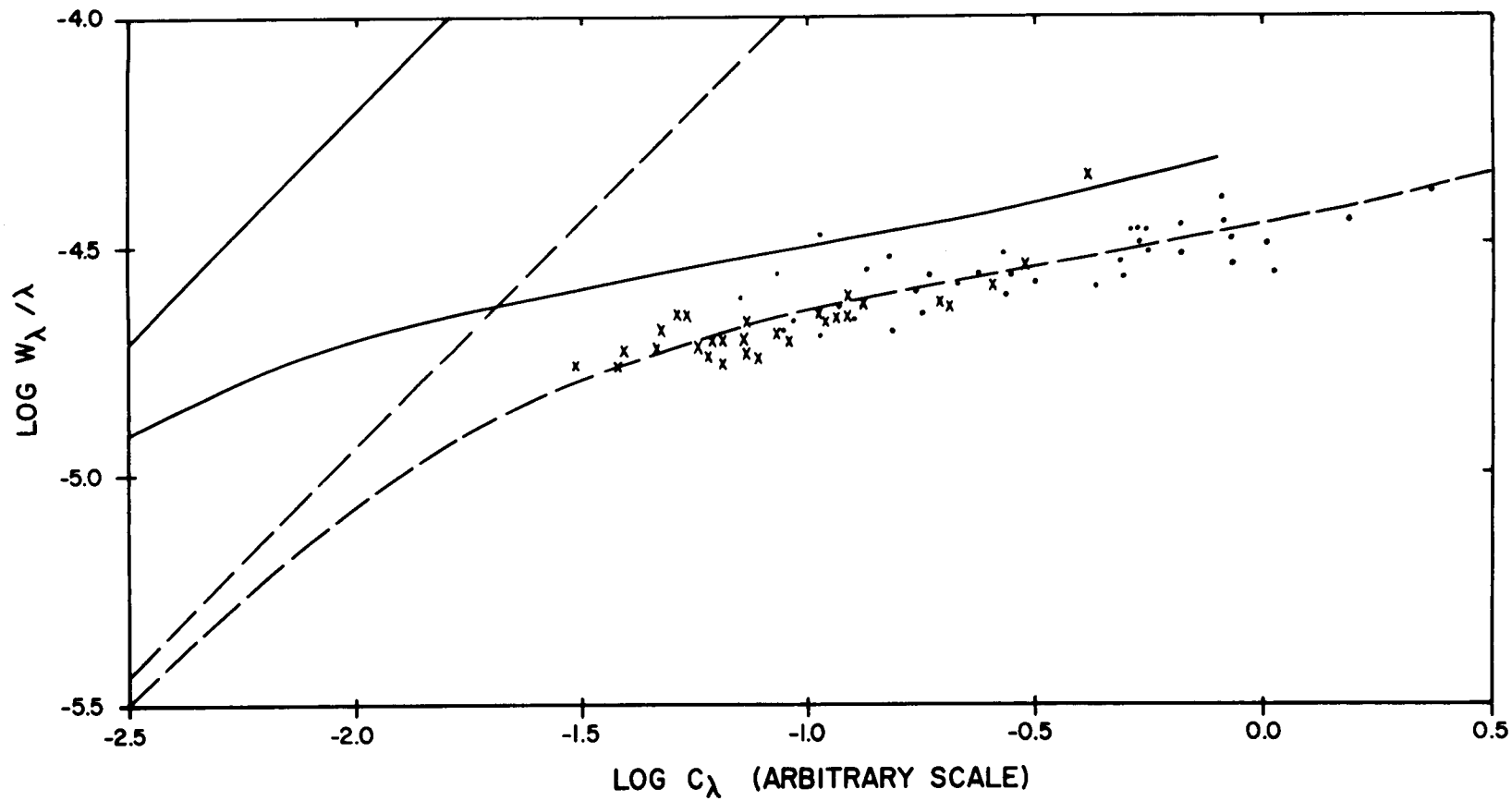
-4.0
-4.5
-5.0
-5.5
LOG W_λ / λ
-2.5
-2.0
-1.5
-1.0
-0.5
0.0
0.5
LOG C_λ (ARBITRARY SCALE)

Fig. 6 Curves-of-growth computed for several values of I_L/I_C (λ = 3500 Å).

Solid Line: $I_L/I_C = 1.0$

Dot-dash Line: $I_L/I_C = 0.7$

Long dash Line: $I_L/I_C = 0.5$

Short dash Line: $I_L/I_C = 0.3$

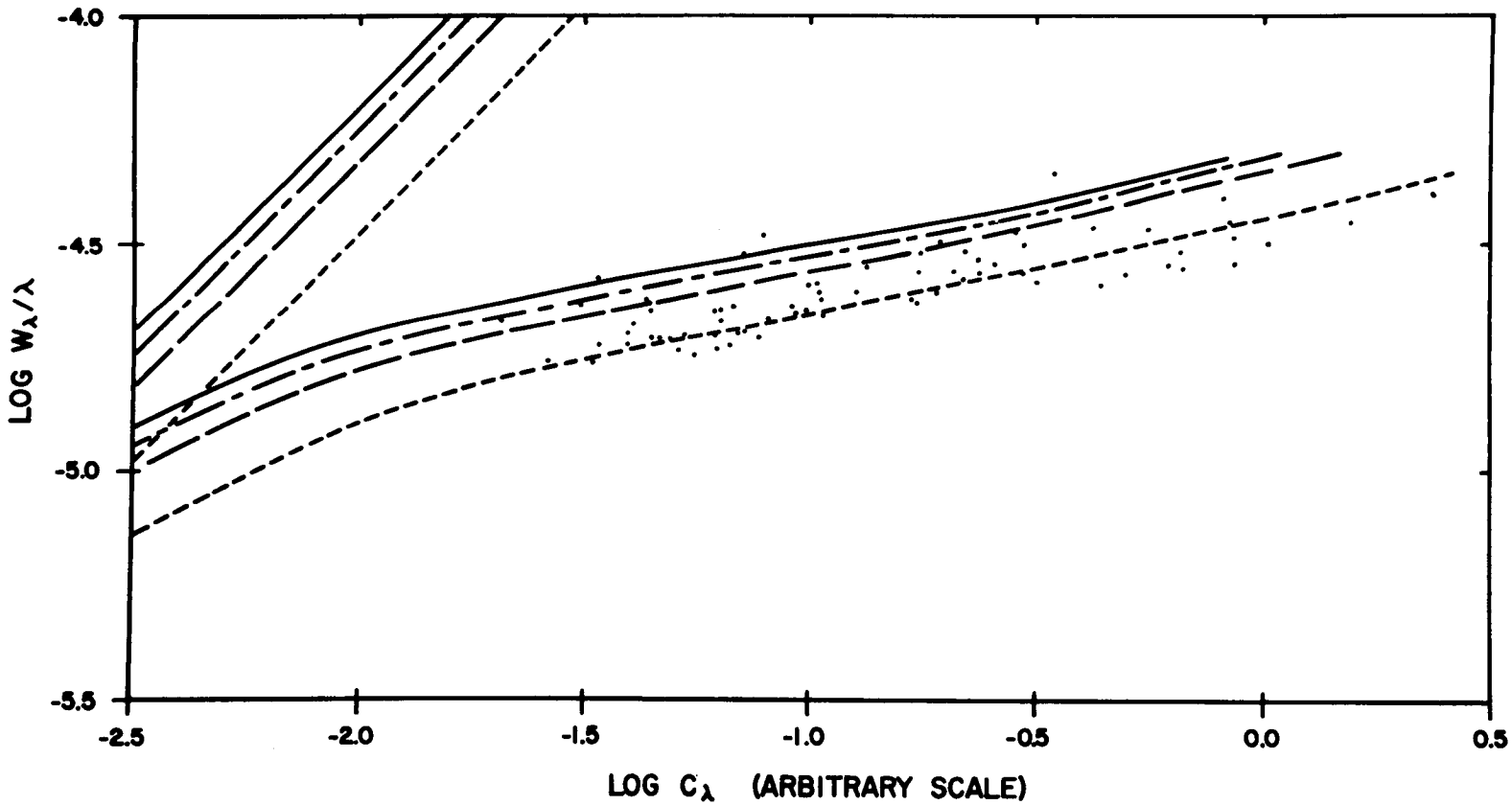
-4.0
-4.5
-5.0
-5.5
LOG W_λ/λ
-2.5
-2.0
-1.5
-1.0
-0.5
0.0
0.5
LOG C_λ (ARBITRARY SCALE)

Fig. 7. Curves-of-growth computed for several values of $(Z+s)^2$.

Solid Line: $(Z+s)^2 = 4$

Dot-dash Line: $(Z+s)^2 = 30$

Dashed Line: $(Z+s)^2 = 120$

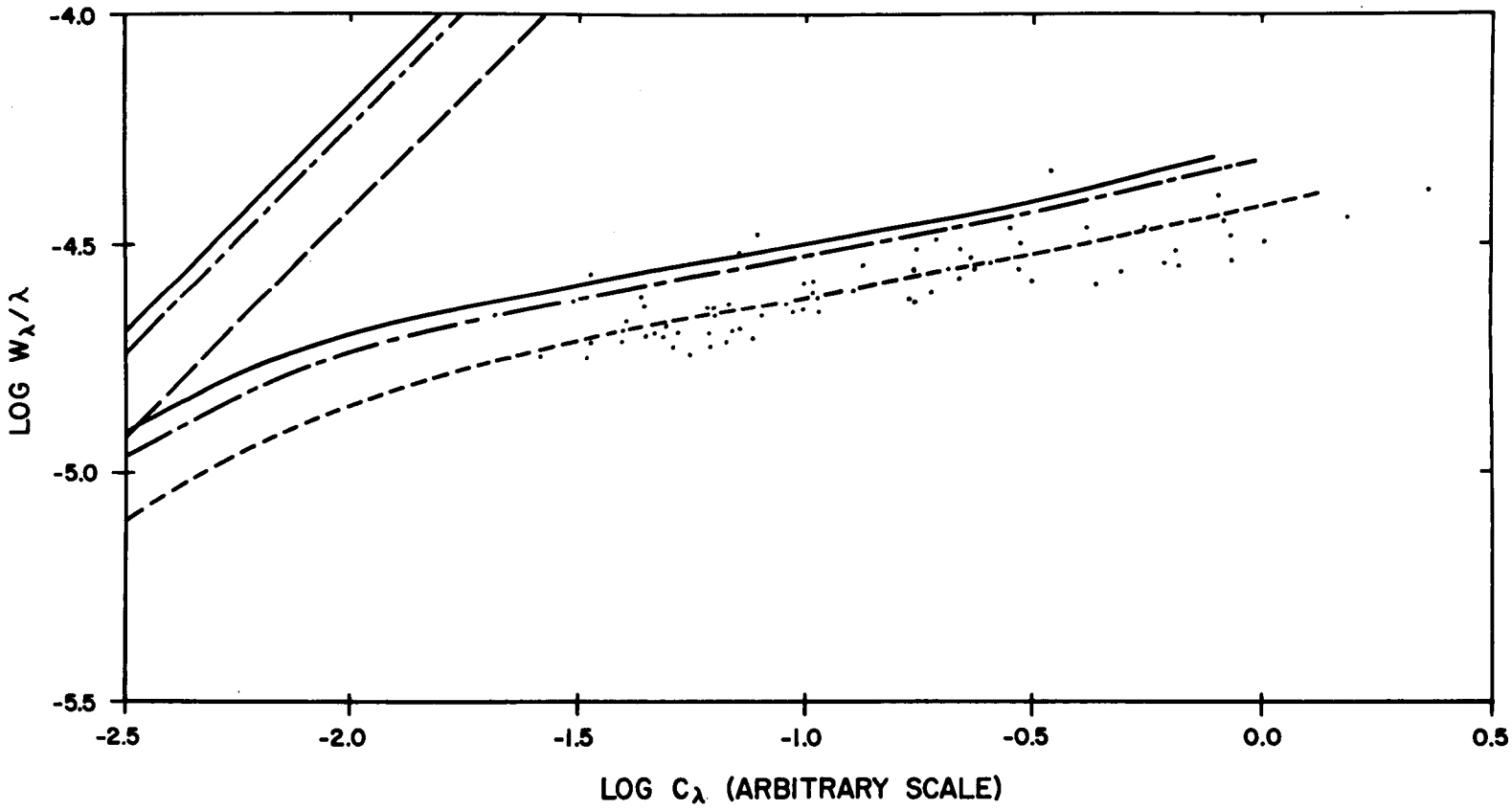
-4.0
-4.5
-5.0
-5.5
LOG W_λ/λ
-2.5
-2.0
-1.5
-1.0
-0.5
0.0
0.5
LOG C_λ (ARBITRARY SCALE)

Fig. 8. A comparison between the observed central intensities of the UV Fe I lines and the intensities computed for opacity models with different values of $(Z+s)^2$.

Points: observations

Solid Line: $(Z+s)^2 = 4$

Dot-dash Line: $(Z+s)^2 = 30$

Dashed Line: $(Z+s)^2 = 120$

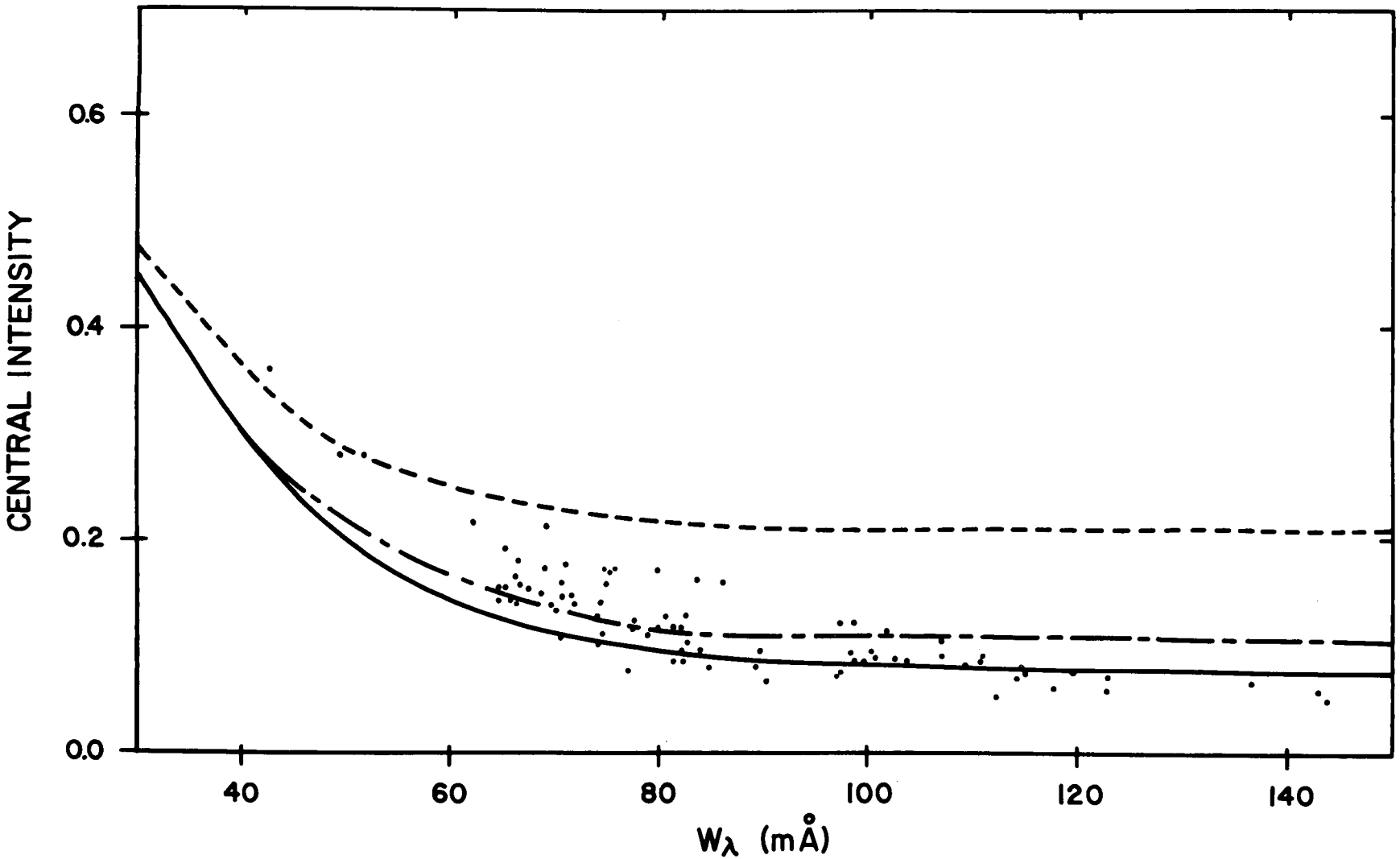
CENTRAL INTENSITY
0.6
0.4
0.2
0.0
40
60
80
100
120
140
Wλ (mÅ)

Fig. 9. The center-limb variation of a typical UV Fe I line as predicted for opacity models with different values of $(Z+s)^2$.

Solid Line: $(Z+s)^2 = 4$

Dot-dash Line: $(Z+s)^2 = 30$

Dashed Line: $(Z+s)^2 = 120$

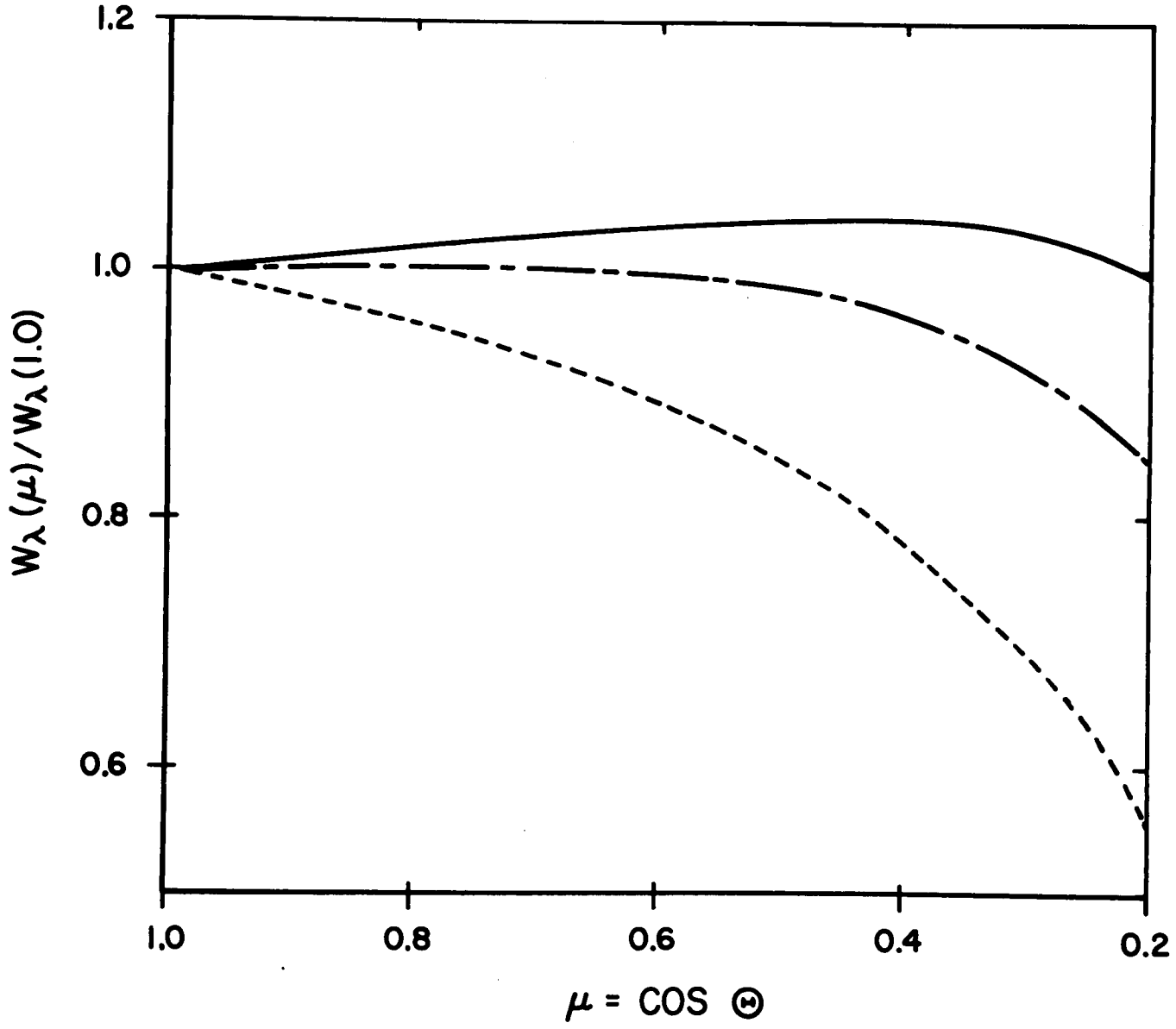
1.2
1.0
0.8
0.6
$W_\lambda(\mu)/W_\lambda(1.0)$
1.0
0.8
0.6
0.4
0.2
$\mu = \cos\Theta$